

---

Masters Theses

Student Theses and Dissertations

---

Spring 2010

## Field analysis of photovoltaic ultracapacitor energy storage system

Jenna Vujic

Follow this and additional works at: [https://scholarsmine.mst.edu/masters\\_theses](https://scholarsmine.mst.edu/masters_theses)



Part of the [Geological Engineering Commons](#)

Department:

---

### Recommended Citation

Vujic, Jenna, "Field analysis of photovoltaic ultracapacitor energy storage system" (2010). *Masters Theses*. 113.

[https://scholarsmine.mst.edu/masters\\_theses/113](https://scholarsmine.mst.edu/masters_theses/113)

This thesis is brought to you by Scholars' Mine, a service of the Missouri S&T Library and Learning Resources. This work is protected by U. S. Copyright Law. Unauthorized use including reproduction for redistribution requires the permission of the copyright holder. For more information, please contact [scholarsmine@mst.edu](mailto:scholarsmine@mst.edu).

FIELD ANALYSIS OF PHOTOVOLTAIC ULTRACAPACITOR ENERGY STORAGE  
SYSTEM

by

JENNA SUE VUJIC

A THESIS

Presented to the Faculty of the Graduate School of the  
MISSOURI UNIVERSITY OF SCIENCE AND TECHNOLOGY

In Partial Fulfillment of the Requirements for the Degree  
MASTER OF SCIENCE IN GEOLOGICAL ENGINEERING

2010

Approved by

Dr. Andrew Curtis Elmore, Advisor  
Dr. Jeffrey Cawlfeld  
Dr. Mariesa Crow



## **PUBLICATION THESIS OPTION**

The purpose of Sections 1-3 is to provide detail beyond that presented in the journal manuscript which is included on pages 13-33. The paper in this thesis is intended for submittal as a journal article in the IEEE Transactions on Sustainable Energy. Section 4 contains supplementary additions to this submittal and has been added for purposes normal to thesis writing.

## ABSTRACT

In the field of innovative power sources, photovoltaics are playing an important role as a clean energy source. Because performance is dependent on instantaneous weather conditions, all stand alone photovoltaic (PV) systems require an energy storage device. Batteries are not suitable for PV source applications due to depth of discharge restrictions, maintenance requirements and minimal power density availability. However, ultracapacitors (UCAPs) have a high power density, require little maintenance, and can be used in sequence with a dc-dc converter to maintain power output at an increased depth of discharge. This paper describes a PV-UCAP power system used to collect and compare solar radiation dependent charge rates over two voltage ranges: the traditional battery range from 35V to 48V and a longer, UCAP-specific range from 13V to 48V. A dataset of 800 charge cycles over 10 days was collected and analyzed. Using the Mann-Whitney hypothesis test, we found that the charge rates collected over the smaller voltage range are systematically different from the charge rates collected over the larger voltage range. The following three methods were used to estimate the variable instantaneous solar radiation during a given charge cycle: Simple Model of the Atmospheric Radiative Transfer of Sunshine Version 2.9.5 (SMARTS) method, vector angle of incidence (*i* vector) method, and direct beam solar radiation on collector ( $I_{bc}$ ) method. The  $I_{bc}$  method shows the best correlation between charge rate and solar radiation estimation. The SMARTS method is preferred over the *i* vector method.

## ACKNOWLEDGEMENTS

I would like to thank Dr. Curt Elmore, Jerry Tichenor, Dr. Jeffrey Cawlfeld, and Dr. Mariesa Crow for their continued support and encouragement throughout my research experience at Missouri S&T. I would also like to thank Samantha DiCenso and Katrina Nolte for the long hours they spent patiently collecting data.

Lastly, I'd like to thank my fellow grad-students for providing much needed comic relief and distraction during times of frustration.

## TABLE OF CONTENTS

	Page
PUBLICATION THESIS OPTION .....	iii
ABSTRACT .....	iv
ACKNOWLEDGEMENTS.....	v
LIST OF FIGURES .....	viii
LIST OF TABLES.....	ix
 SECTION	
1. INTRODUCTION.....	1
2. EXPERIMENTAL DESIGN AND WORK NARRATIVE .....	2
3. OBJECTIVES AND GOALS.....	5
 PAPER	
ANALYSIS OF STAND-ALONE PV-UCAP ENERGY STORAGE SYSTEM .....	6
Abstract.....	6
Introduction .....	7
System Description.....	8
Methods .....	9
Results and Discussion .....	13
Conclusions .....	18
References .....	18
 SECTION	
4. RECOMMENDATIONS FOR FUTURE WORK .....	26

APPENDIX .....	27
REFERENCES .....	28
VITA.....	29

**LIST OF FIGURES**

	Page
Figure 1: System description .....	19
Figure 2: Definition of $i$ vector.....	19
Figure 3: Definition of solar angles.....	20
Figure 4: Raw UCAP output voltage.....	20
Figure 5: Raw UCAP voltage data troughs and peaks. ....	21
Figure 6: UCAP voltage start and end points for defined charge cycle .....	21
Figure 7: Long range $I_{bc}$ scatterplot.....	22
Figure 8: Long range $I_{bc}$ scatterplot using $y/x$ transformation. ....	22
Figure 9: Long range $i$ vector normal probability plot .....	23

**LIST OF TABLES**

	Page
Table I: System charge behavior .....	23
Table II: SMARTS input data .....	24
Table III: System sensor gains and offsets .....	24
Table IV: 2009 charge cycle statistics .....	25

## SECTION

### 1. INTRODUCTION

Photovoltaic (PV) units are popular, solid state renewable energy source for stand-alone systems due to range of application and increasing affordability. PV power source systems commonly depend on batteries to store and supply intermittent energy collected by the PV unit. A standard lead acid battery costs less per joule per unit energy, has a higher energy density, and sets precedent over an ultracapacitor (UCAP) for PV source applications. UCAPs are designed to last the life of the system, require minimal maintenance, tolerate a wide range of temperature variation, and are less sensitive to depth of discharge and charge/discharge rates than the conventional lead acid battery. Several recent studies suggest coupling a UCAP and a lead acid battery to form a hybrid system well suited to store an adequate amount of energy while providing more power. Glavin and Hurley (2007) describe UCAPs as having a greater power density and temperature tolerance than a typical lead acid battery and propose a hybrid system to take advantage of both technologies while increasing the efficiency of the system. More specifically, the UCAP is used to charge the battery when additional power is provided by the PV unit and decreases required battery capacitance by supplying peak power. Glavin et al. (2008) incorporated an energy control unit to the hybrid system and expect that adding a UCAP will increase the State of Charge (SOC) of the batteries for peak and pulse current loads.

## 2. EXPERIMENTAL DESIGN AND WORK NARRATIVE

The initial phase of the research was to trouble shoot the equipment and collect usable field data. The system weighed approximately 200 pounds and was mounted to a small wagon to be transported to and from the field location daily. The following steps had to be taken in order to begin collecting data:

- Photovoltaic panels connected in series and parallel to the DC bus
- Voltage and current sensors connected to the datalogger as described by the PC400 wiring diagram
- Connect computer to datalogger to ensure datalogger is set to properly record and store collected data, and to ensure that all sensor are functional

A document containing the standard operating procedure can be found in the appendices.

The system is operated manually and requires at least one person present at all times to switch the inverter and PV unit on and off. Two undergraduate students were trained to properly time the system switching to collect the data needed. Approximately 2 weeks were spent troubleshooting the system and weather station sensors. A thermal couple sensor was set up to collect PV panel modular temperature; unfortunately, the data collected was not useful during the data analysis phase. A second pyranometer was mounted at an angle equal to the panel tilt. This data was used to verify values calculated from empirical equations used to adjust horizontal pyranometer data for panel tilt. An additional 2 weeks was spent collecting charge cycles using 2, 4, and 6 panels rather than the total 8 panel array.

Approximately 2 weeks were spent manipulating the system to discharge to 10V in order to collect charge rates over the long range. Initially, the system would allow the UCAP to discharge to 40V. Once the charge controller was set to protect a 12V battery rather than a 48V battery from discharging, the system would allow the UCAP to discharge to 20V before the inverter shut off. A dc-dc converter was added to boost the outgoing UCAP current, allowing the UCAP to fully discharge to 10V. Two weeks of usable data were then collected. The data was stored as a text file at the end of every day the system was in operation. The system was shut down in the case of rain.

The second phase of the research was analyzing the data. The following data was collected on 5 second intervals: ambient temperature, modular temperature, PV current, PV voltage, solar radiation, and wind speed. Spreadsheets were designed to calculate the average solar radiation and charge rate per charge cycle. Initially, a charge cycle was defined as the difference between a trough and peak in the UCAP voltage sensor data. This method incorrectly identified discharge voltage fluctuations as charge cycles. The charge cycles were redefined, as described in the paper, to incorporate fixed ranges as charge cycle start and end points. By requiring a charge cycle to start within a fixed range, some collected charge cycles were not analyzed due to sampling frequency. For example, when the UCAP is charged 35V over approximately 1 minute, sampling every 5 seconds is not frequent enough to detect when the UCAP voltage charges through a 2V start point range.

The experimental design did not account for random factors that vary daily, like temperature. To account for this variation, charge rates through the short range

were extracted from the long range and compared to the long range data for a given day. The 2-sample Mann-Whitney hypothesis test was used to support the argument that the short range charge rates extracted from the long range were comparable to the charge rates collected when the UCAP was charged through the short range. The 2-sample Mann-Whitney hypothesis test was used to determine that the extracted short range charge rates were systematically different from the long range charge rates for a given day.

The correlation between the response variable, the charge rate, and the predictor variable, the estimated solar radiation, was analyzed using scatterplots. A probability distribution could not be identified for the charge rate data due to high variability. The data was transformed by dividing the charge rate by the estimated solar radiation. A normal distribution was the best fit for the transformed long range data.

### 3. OBJECTIVES AND GOALS

The objective of this research is to compare field-collected UCAP charge rates as a response to variable solar radiation over two ranges: the first one is the traditional voltage range over which a 48V battery is charged and the second is the voltage range afforded by UCAP. To compare UCAP charge rate as a function of solar radiation and voltage range over which the UCAP is charged, we felt it appropriate to evaluate three methods to account for the variable instantaneous solar radiation during a given charge cycle: Simple Model of the Atmospheric Radiative Transfer of Sunshine Version 2.9.5 (SMARTS) method, vector angle of incidence ( $i$  vector) method, and direct solar radiation on collector ( $I_{bc}$ ) method.

## PAPER

### ANALYSIS OF A STAND-ALONE PV-UCAP ENERGY STORAGE SYSTEM

Index terms: photovoltaics, ultracapacitor, energy storage, renewable energy

Byline: Jenna Vujic<sup>1</sup>; Andrew Elmore<sup>2</sup>; Mariesa Crow<sup>3</sup>; Jeffrey Cawlfild<sup>4</sup>

Author contact information: Geological Engineering, Missouri University of Science & Technology, 125 McNutt Hall, Rolla, MO 65409. Telephone (573) 341-6784, Fax (573) 341-6935, email [jstpkd@mst.edu](mailto:jstpkd@mst.edu)

### Abstract

In the field of innovative power sources, photovoltaics are playing an important role as a clean energy source. Because performance is dependent on instantaneous weather conditions, all stand alone photovoltaic (PV) systems require an energy storage device. Batteries are not suitable for PV source applications due to depth of discharge restrictions, maintenance requirements and minimal power density availability. However, ultracapacitors (UCAPs) have a high power density, require little maintenance, and can be used in sequence with a dc-dc converter to maintain power output at an increased depth of discharge. This paper describes a PV-UCAP power system used to collect and

---

<sup>1</sup> Department of Geological Engineering, Missouri University of Science & Technology, 129 McNutt Hall, Rolla, MO 65409, USA (email: [jstpkd@mst.edu](mailto:jstpkd@mst.edu)).

<sup>2</sup> Department of Geological Engineering, Missouri University of Science & Technology, 129 McNutt Hall, Rolla, MO 65409, USA (email: [elmoreac@mst.edu](mailto:elmoreac@mst.edu)).

<sup>3</sup> Department of Computer and Electrical Engineering, Missouri University of Science & Technology, 305 McNutt Hall, Rolla, MO 65409, USA (email: [crow@mst.edu](mailto:crow@mst.edu)).

<sup>4</sup> Department of Geological Engineering, Missouri University of Science & Technology, 129 McNutt Hall, Rolla, MO 65409, USA (email: [jdc@mst.edu](mailto:jdc@mst.edu)).

compare solar radiation dependent charge rates over two voltage ranges: the traditional battery range from 35V to 48V and a longer, UCAP-specific range from 13V to 48V. A dataset of 800 charge cycles over 10 days was collected and analyzed. Using the Mann-Whitney hypothesis test, we found that the charge rates collected over the smaller voltage range are systematically different from the charge rates collected over the larger voltage range. The following three methods were used to estimate the variable instantaneous solar radiation during a given charge cycle: Simple Model of the Atmospheric Radiative Transfer of Sunshine Version 2.9.5 (SMARTS) method, vector angle of incidence ( $i$  vector) method, and direct beam solar radiation on collector ( $I_{bc}$ ) method. The  $I_{bc}$  method shows the best correlation between charge rate and solar radiation estimation. The SMARTS method is preferred over the  $i$  vector method.

## Introduction

Photovoltaic (PV) units are a popular, solid state renewable energy source for stand-alone power systems due to range of application and increasing affordability. However, an energy storage method is required to bridge inherent power fluctuations due to weather variability. PV power source systems commonly depend on a battery system to store and supply intermittent energy collected by the PV unit [1]. The standard lead acid battery costs less per unit energy, has a higher energy density, and sets precedent over the ultracapacitor (UCAP) for PV source applications. On the other hand UCAPs are designed to last the life of the system, require minimal maintenance, tolerate a wide range of temperature variation, and are less sensitive to depth of discharge and charge/discharge rates than the traditional lead acid battery [2]. Several recent studies suggest coupling a

UCAP and a lead acid battery to form a hybrid system is well-suited to store an adequate amount of energy while providing more power. More specifically, a UCAP is used to charge the battery when additional power is provided by the PV unit and decreases required battery capacitance by supplying peak power [3]. However, energy density becomes less of a necessity when the system is not required to sustain power over night. For example, a study in 2009 used a UCAP to store energy collected by both a PV unit and wind turbine to power a water disinfection unit [4]. In this case, batteries are an undesirable storage method due to maintenance requirements, storage sensitivities, and increased weight.

The main objective of this paper is to compare field-collected UCAP charge rates as a response to variable solar radiation over two ranges: the first one is the traditional voltage range over which a 48V battery is charged and the second is the voltage range afforded by UCAP. To compare UCAP charge rate as a function of solar radiation and voltage range over which the UCAP is charged, we felt it appropriate to evaluate three methods to account for the variable instantaneous solar radiation during a given charge cycle: Simple Model of the Atmospheric Radiative Transfer of Sunshine Version 2.9.5 (SMARTS) method, vector angle of incidence ( $i$  vector) method, and direct solar radiation on collector ( $I_{bc}$ ) method.

## System Description

This paper describes a system which consists of the following standard components as described in Fig. 1: PV array, charge controller, storage device, and inverter. An UCAP was chosen as the storage device instead of the traditional lead acid battery. The system is not intended to operate through the night; therefore, minimal

maintenance cost is valued over the added energy density gained by pairing a UCAP with a battery. In order to take advantage of the added power density afforded by the UCAP, the MX60 charge controller is set for a 12V battery system rather than 48V battery system. This increased the depth of discharge by 10-12V. The bulk and float maximum power points (FMPPT and BMPPT) were set at 48V. The charge controller is designed to increase the efficiency of the system by using maximum power point tracking while prolonging the lifetime of the battery by regulating the rate and depth of discharge. The system charge behavior is described in Table I. When the power supplied by the PV array is equal to the power required by the load, power is supplied to the load independent of the UCAP's state of charge. When the PV array produces more power than required by the load, the additional power is used to charge the UCAP as needed. A Campbell Scientific CS1000 datalogger was used to record all data from the following individual instruments: Campbell Scientific CS300 pyranometer used to collect solar radiation horizontal to the earth's surface, two LEM LV-25 P voltage sensors to measure UCAP and PV output voltages, and two F.W. Bell CLN-50 current sensors to measure UCAP and PV output currents.

## Methods

The system was setup at latitude 37.956 north and longitude 91.777 west and operated during daylight hours when no precipitation was present. The PV array was mounted facing due south at a tilt angle of 23 degrees, 15 degrees less than site latitude to optimize output during the summer season [5]. System operators manually controlled when the PV unit was permitted to charge the UCAP. Without a converter to boost the UCAP output voltage, the inverter would interrupt UCAP discharge at 34-36V. For this

reason, charging the UCAP from 34-36V to 47-49V became the short voltage range comparable to the range over which the charge controller would regulate a 48V battery system. A dc-dc converter was added to boost the UCAP output voltage, allowing the UCAP to discharge over a larger range without inverter-based interruption. Because the MX60 requires at least 10.5V on the battery input terminals, operators would manually turn off the inverter once the UCAP discharged to  $13\pm 1V$ . The remaining charge supplied power to the charge controller until the PV unit was able to begin re-charging the UCAP. Charging the UCAP from  $13\pm 1V$  to  $48\pm 1V$  became our longer charge rate which takes advantage of the UCAP's discharging insensitivities. Both charge rates were calculated using UCAP voltage data collected by the datalogger at 5 second intervals. To account for inconsistency introduced by operators manually switching the equipment off and on, the charge cycles were defined by the UCAP voltage level and not by the time at which the operator flipped the switch. To account for the presence of random effects due to environmentally variability from one day to the next, a short range charge rate was extracted from the long range charge rate data to be used as a means of comparison.

Ten charge cycles were collected in the laboratory to establish a baseline. Charging the UCAP using a *Sorensen DHP Series* constant power source was intended to identify charge rate variability inherent to the system itself rather than environmental conditions.

The charge rate is dependent on the amount of instantaneous solar radiation exposed to the PV array. Global instantaneous solar radiation consists of three components: direct, diffuse, and reflected [6]. Each of the three methods used account for varying levels of diffuse and reflected solar radiation. The SMARTS method calculates

clear sky global tilt irradiance (GTI) for a given time and location. The  $i$  vector method uses a geometric spreadsheet-based model to calculate sun angles independent of site-specific random data. The  $I_{bc}$  method is dependent on the solar radiation data collected by the pyranometer and adjusted for the tilt angle of the PV array.

SMARTS was developed by Dr. Christian Gueymard to calculate solar direct beam irradiance for a cloudless atmosphere, incorporating diffuse and reflected solar radiation [6]. Table II contains the input data used to calculate GTI for each charge cycle. Card 17a outputs expected GTI per charge cycle to a fixed format text file. Each value must then be exported manually from the text file to a spreadsheet to be used for further analysis. This method was most labor intensive relative to the other two methods used.

The  $i$  vector method is a geometric model used to calculate the angle vector at which the total instantaneous direct beam solar radiation would hit the pyranometer on a cloudless day independent of diffuse and reflected solar radiation. The  $i$  vector solar radiation estimation is easily calculated using a spreadsheet. The  $i$  vector is equal to the cosine of the angle of incidence,  $i$ , of beam radiation on a surface and will take on values between 0 and 1 as illustrated in Fig. 2. Equations (1) through (8) show how  $i$  vector is related to the solar angles illustrated in Fig. 3 [7].

Eq. (1) shows the declination angle,  $\delta$ , as the angle of deviation from the sun to directly above the equator and is a function of  $n$ , the ordinal date.

$$\delta = 23.45^\circ \sin \left[ \frac{360^\circ (284 + n)}{365^\circ} \right] \quad (1)$$

The solar hour angle,  $hs$ , is the difference between solar noon and the position of the sun. Each solar hour represents 15 degrees as shown in Eq (2).

$$hs = 15^\circ(\text{hours from local solar noon}) \quad (2)$$

The Equation of Time,  $ET$ , is a correction factor to account for the irregularity of the speed of the earth around the sun.

$$ET(\text{in minutes}) = 9.87 \sin 2 B - 7.53 \cos B - 1.5 \sin \frac{360^\circ(n-81)}{364^\circ} \quad (3)$$

The relationship between local standard time (LST) and solar time is shown in Eq (4).  $Long_{st}$  is the standard time meridian while  $long_{local}$  is the on-site, local longitude.

$$\text{Solar Time} = LST + ET + (Long_{st} - Long_{local}) \cdot 4 \left( \frac{\text{min}}{\text{degree}} \right) \quad (4)$$

The altitude angle,  $\alpha$ , is a function of the local latitude,  $lat$ , the declination angle, and the solar hour angle.

$$\sin \alpha = \sin Lat \sin \delta + \cos Lat \cos \delta \cos hs \quad (5)$$

The solar azimuth,  $az$ , is the function of the declination angle, solar hour angle, and altitude angle.

$$\sin az = \cos \delta \sin hs / \cos \alpha \quad (6)$$

The  $i$  vector is equal to  $\cos i$  as shown in Fig. X.

$$\cos i = \cos \alpha \cos az \sin \beta + \sin \alpha \cos \beta = \sin \alpha \quad (7)$$

$I_{bc}$  is a method that uses the solar radiation data collected at horizontal by the pyranometer to determine the total solar radiation striking the PV array at a tilt angle of  $\beta$

which was 23 degrees for this project. The angle of incidence,  $I$ , is used to calculate the beam radiation on the collector [3] as shown by Eq. (8).

$$I_{bc} = I_{bN} \cos i \quad (8)$$

When the collector is horizontal,  $\beta = 0$  and Eq (8) simplifies to Eq (9).

$$\cos i = \sin \alpha \quad (9)$$

The beam radiation,  $I_{bh}$ , is equal to  $I_{bc}$  for the horizontal collector. Therefore,  $I_{bN}$  is a function of  $I_{bh}$  and  $\sin \alpha$  for a tilted collector as shown in Eq. (10).

$$I_{bN} = \frac{I_{bh}}{\sin \alpha} \quad (10)$$

This value of  $I_{bN}$  is used in Eq. (8) to calculate  $I_{bc}$  for the solar array tilted at  $\beta = 23^\circ$ .

This method was expected to show high correlation to the measured charge rate as it is a function of cloud-dependent field data. The  $I_{bc}$  method is most sensitive as the pyranometer data accounts for all forms of solar radiation including instantaneous cloud conditions. The *i vector* method is the least sensitive method as it does not account for random, environmental effects.

## Results and Discussion

Short range data were collected for 5 days beginning June 29<sup>th</sup>, 2009. Long range data were collected for 5 days beginning July 28<sup>th</sup>, 2009. The system sensor data was corrected for gains and offsets shown in Table III. The system was charged using a clean power source to establish a baseline and recognize charge rate variability inherent to the technology used. The UCAP was charged 10 times through the long voltage range and

short range data were extracted. The resulting long range charge rate data set had coefficient of variance equal to 0.02. Field-collected long range charge cycles collected on August 15<sup>th</sup>, 2009 had a coefficient of variance equal to 0.32. The resulting extracted short range data set had a coefficient of variance equal to 0.02. Field-collected extracted short range charge cycles collected on August 15<sup>th</sup>, 2009 had a coefficient of variance equal to 0.39. Both long and short range data sets collected in the laboratory were compared to a dataset with a normal distribution to determine goodness-of-fit. The following respective p-values were calculated: 0.045 and 0.693.

Fig. 4 shows the raw UCAP output voltage data collected every five seconds for one discharge cycle and one charge cycle. Small voltage fluctuations during the discharge cycles are present due to the result of switching during rapid discharge. Fig. 5 shows the UCAP's long range voltage troughs and peaks. As shown, the troughs vary through 1.89-16.56V due to discharge voltage fluctuations and the sampling frequency. The peaks vary through 40.77-54.06V due mostly to sampling frequency as the charge controller adjusts the incoming voltage to maintain the set bulk maximum power point (B-MPPT) level. The charge rate for a given charge cycle is defined as shown by equations (10) and (11). This definition both avoids defining discharge voltage fluctuations as charge cycles and provides constant charge cycle start and end points.

$$\text{long range charge rate} = \frac{(V_3 - V_2)}{(t_3 - t_2)} \quad (11)$$

$$\text{extracted short range charge rate} = \frac{(V_3 - V_1)}{(t_3 - t_1)} \quad (12)$$

The voltage start and end points were fixed ranges to account for instantaneous rate changes: the start point must be  $12 \pm 1V$  followed by increasing voltage, while the

end point must be within  $48 \pm 1V$  preceded by a lower voltage for long range charge rates. The short range charge cycle was defined using the same method except the start point was defined as a point that must be within 34-36V followed by increasing voltage. Fig. 6 shows the charge cycle start and end points as defined by equations (11) and (12). The charge cycle start points vary between 11.0-12.9V and the end points vary from 47.0-47.8V due to sampling frequency.

For the 5 days the UCAP charged within the long voltage range, both extracted short range charge rates and long range charge rates were collected. The data were then compared using the 2-sample Mann-Whitney hypothesis test to determine if a systematic difference exists between charge rates that were collected as the UCAP charged through the short range and charge rates that were extracted from the short range as the UCAP charged through the long range. For all 5 days, p-values greater than  $\alpha=0.05$  were calculated using Minitab 15 software assuming the following null and alternative hypothesis:

$$H_0: \text{extracted short range charge cycle } y/x = \text{sampld short range charge cycle } y/x$$

$$H_a: \text{extracted short range charge cycle } y/x \neq \text{sampld short range charge cycle } y/x$$

There is not sufficient evidence to reject  $H_0$  at a 95% confidence interval, meaning the probability of incorrectly rejecting the null hypothesis is high. Given these results, we conclude that the sampled and extracted short range data are from the same population and may be treated as such. By assuming that the sampled and extracted short range data are from the same population, the short range and long range data collected on the same day at the same time (using one system) can then be compared independent of

effects that vary day to day. For each of the 5 days the UCAP charged over the long voltage range, the Mann-Whitney test was used to determine if the charge rate over the long range was systematically different than the charge rate over the short range. There was sufficient evidence to suggest that the small range data are not from the same population as the short range data. The following null and alternative hypotheses were assumed:

$$H_0: \text{short range charge cycle } y/x = \text{long range charge cycle } y/x$$

$$H_a: \text{short range charge cycle } y/x \neq \text{long short range charge cycle } y/x$$

The p-value was 0.00 for all 5 days, meaning there is sufficient evidence to reject  $H_0$ . It was concluded the charge rate over the long range is systematically different than the charge rate from the extracted short range data.

We were unable to fit a probability distribution within a 95% confidence interval to the response variable, the charge rate, over a given day. UCAP charge rates as a function of the solar radiation estimated using the  $I_{bc}$  method showed the best r-squared value of 0.84 for July 31, 2009. The data was transformed by dividing the charge rate by the predictor variable, solar radiation estimate by each of the 3 methods, and then compared to various probability distributions. This  $y/x$  transformation was used to normalize the charge rates to the solar radiation estimates in an effort to characterize the non-homogenous variability found in the data. The transformed data over the long range showed the most useful goodness of fit to a normal distribution. Fig. X shows the probability plot for the long range data on August 14, 2009.

The following  $H_0$  and  $H_a$  were used to determine if there was a systematic difference between the distribution of the data and data having a normal distribution.

$H_0$ : (charge rate / solar radiation) distribution = normal distribution

$H_a$ : (charge rate / solar radiation) distribution  $\neq$  normal distribution

The p-values representing the goodness of fit of the  $y/x$  transformed data collected over the long range to a normal distribution are shown in Table IV.

## Conclusions

As predicted, the charge rate observed when the UCAP is charging over the long voltage range is faster. Allowing the PV unit to charge the UCAP over a longer voltage range does take advantage the power density afforded by the UCAP technology.

The charge rates collected as a function of solar radiation are highly variable. The  $I_{bc}$  Method of estimating solar radiation shows the best correlation between the UCAP charge rates. The SMARTS method is preferred over the  $i$  vector method despite the additional time required to manually input and output data, because the SMARTS data show a stronger correlation between solar radiation present and resulting UCAP charge rate. The long range charge rate is faster on average than the short range data. The baseline data is less variable for both field collected short and long range charge rates. This is expected as the primarily source of variation is assumed to be the inherent variable solar radiation throughout a given day. This research can be used to further investigate power output prediction models for similar energy storage systems in a variety of locations.

## References

- Glavin, M.E. and Hurley, W.G. (2007). Ultracapacitor/battery hybrid for solar energy storage. *Solar Energy*, 30(2), 212-218.
- Glavin, M.E., Chan, P.K.W., Armstrong, S., and Hurley, W.G. (2008). A stand-alone photovoltaic supercapacitor battery hybrid energy storage system. *Solar Energy*, 14, 1003-1016.
- Goswami, D.Y., Kreith, F., and Kreider, J.F. (2000). *Principles of Solar Engineering*. Taylor and Francis Group, LLC, New York, New York.

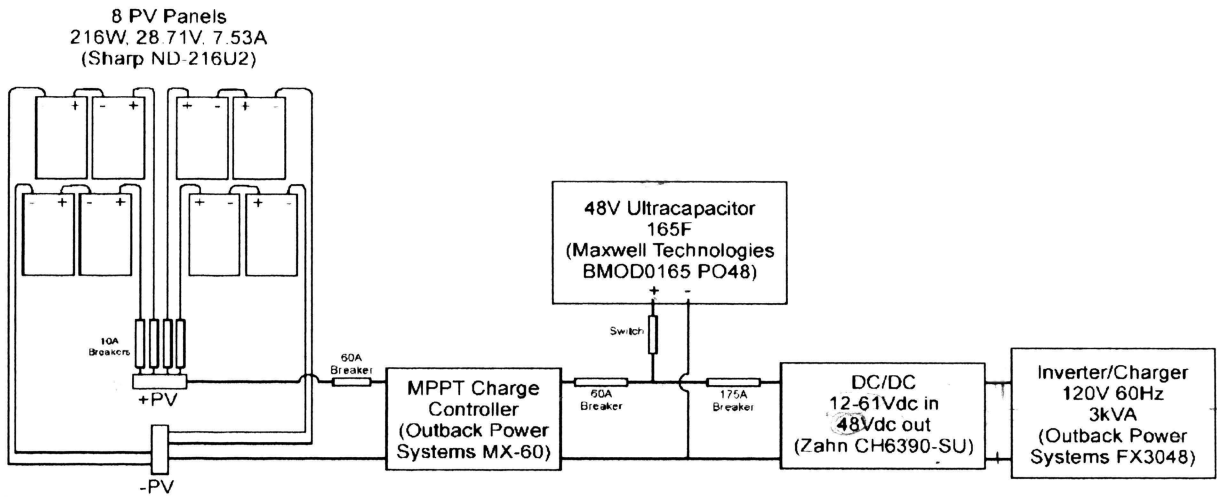


**Figure 1: System description**

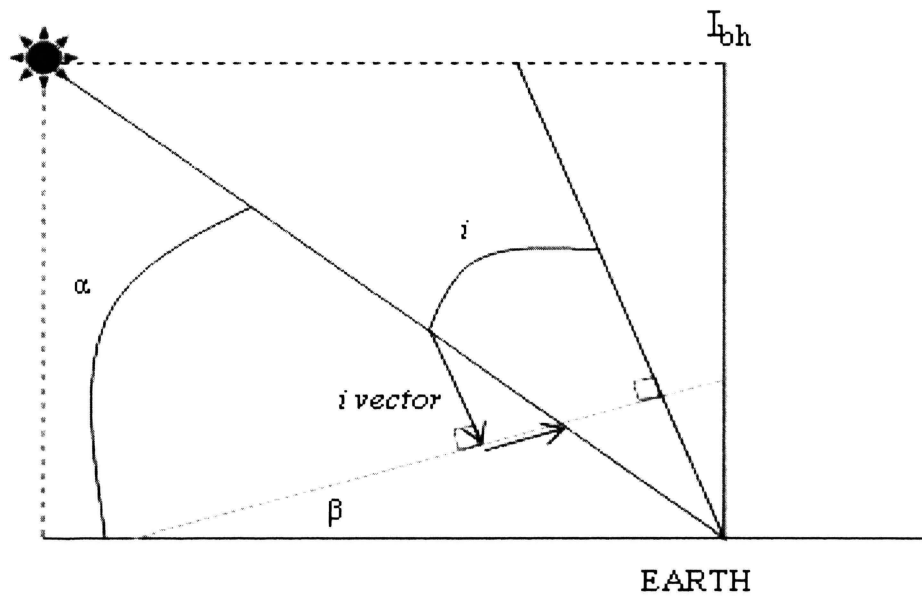


**Figure 2: Definition of *i* vector**

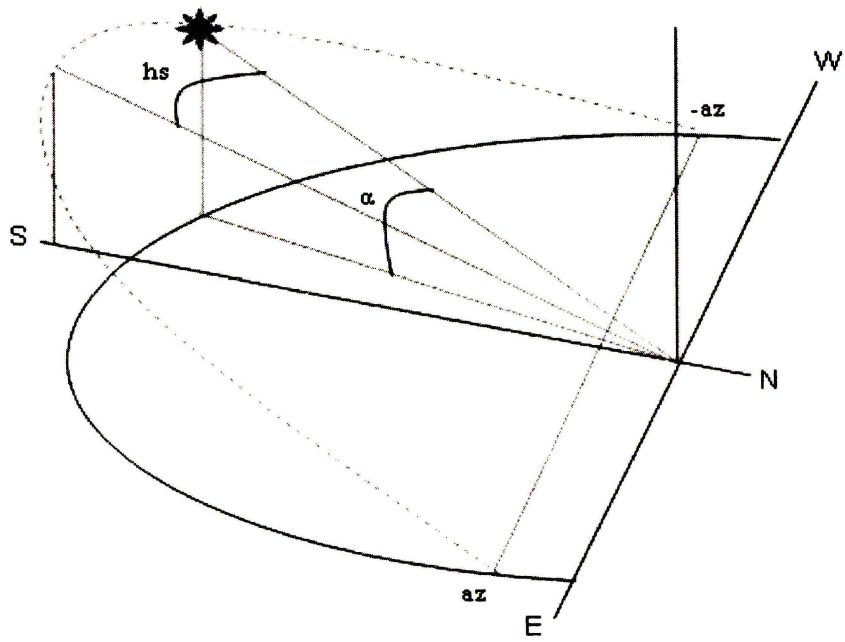


**Figure 3: Definition of solar angles**

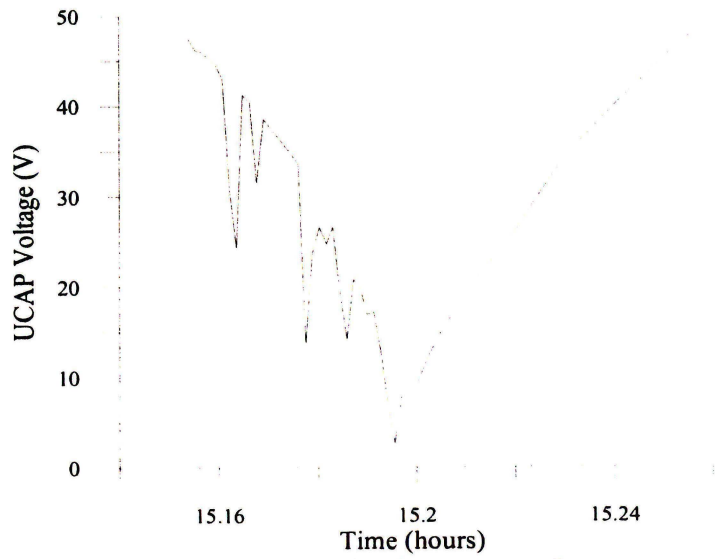


**Figure 4: Raw UCAP output voltage**

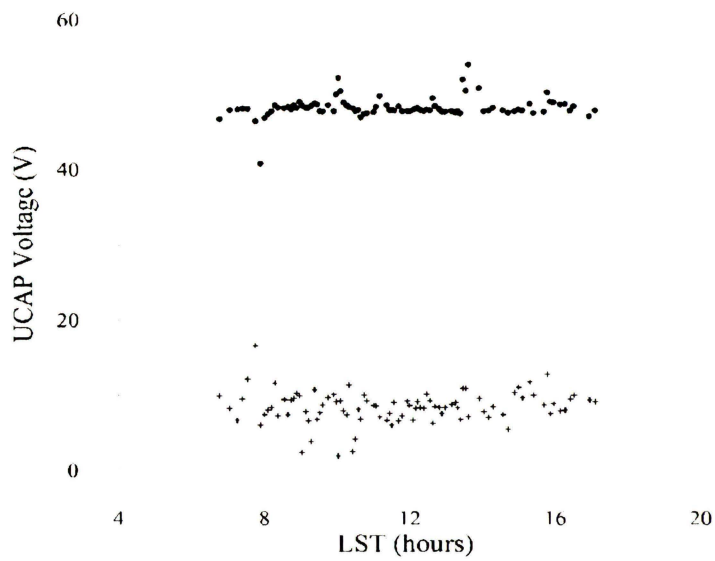


**Figure 5: Raw UCAP voltage troughs and peaks**

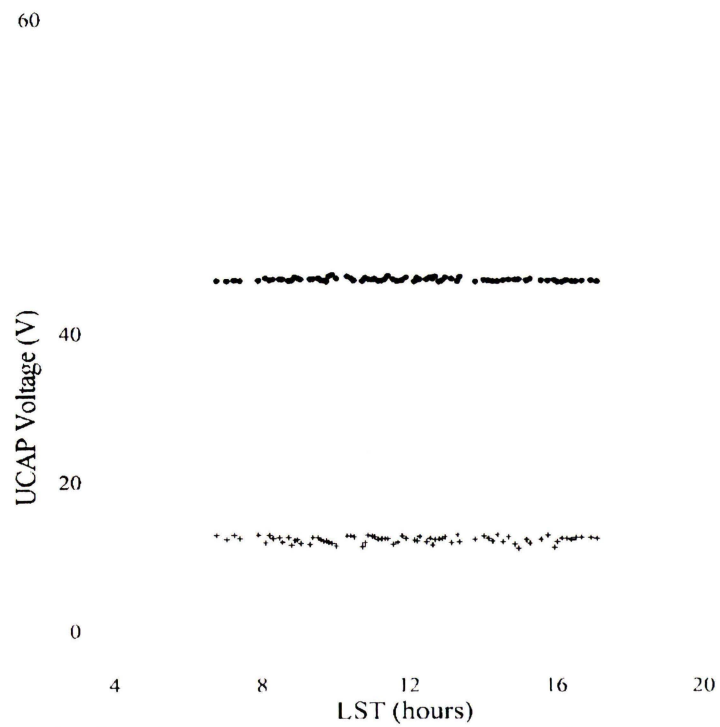


**Figure 6: UCAP voltage start and points for defined charge cycle**

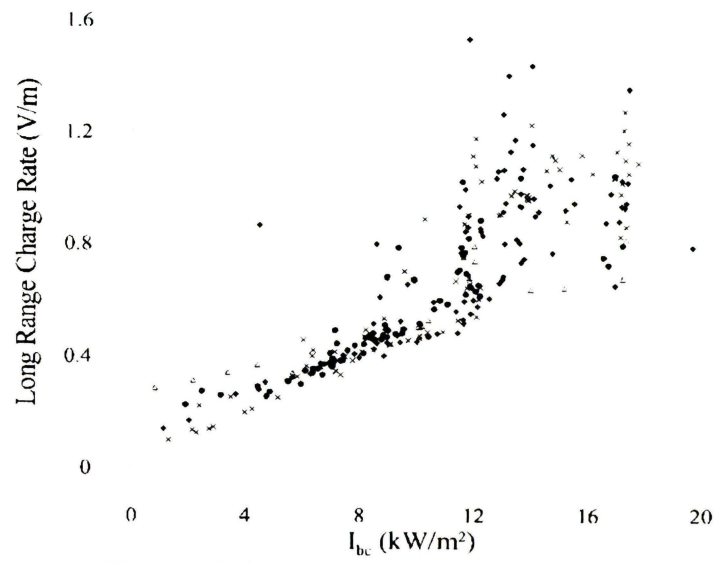


**Figure 7: Long range  $I_{bc}$  scatterplot**

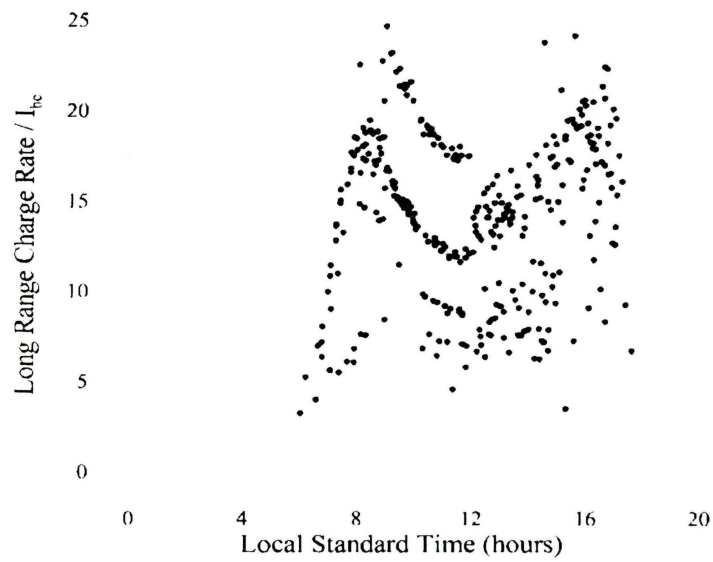


**Figure 8: Long range  $I_{bc}$  scatterplot using y/x transformation**

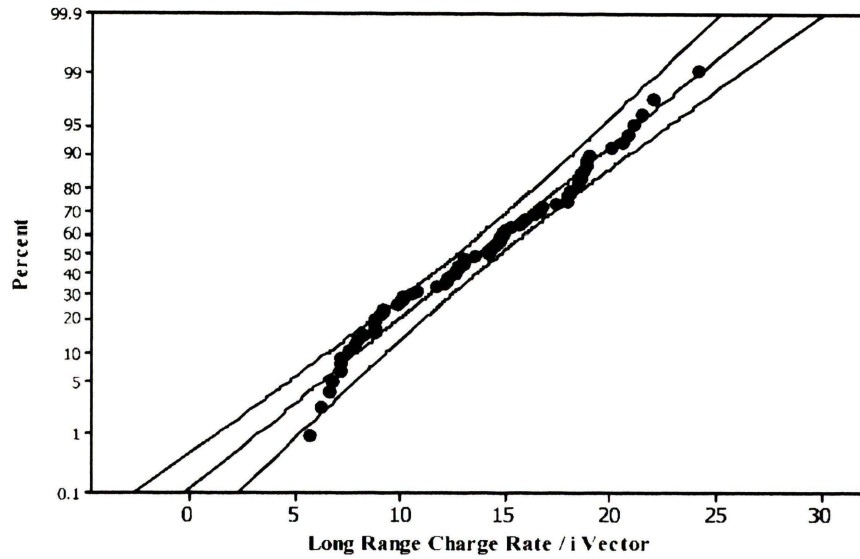


Figure 9: Long range  $i$  vector normal probability plot

Table I: System charge behavior

	<b>UCAP fully charged</b>	<b>UCAP not fully charged</b>	<b>UCAP fully discharged</b>
$P_{pv} = P_L$	PV supplies load	PV supplies load	PV supplies load
$P_{pv} < P_L$	UCAP will supply additional power required	UCAP will supply additional power required	No power will be supplied to load
$P_{pv} > P_L$	PV supplies load	PV supplies load and charges UCAP	PV supplies load and charges UCAP

Table II: SMARTS input data

Card #	Card Name	Input
2a	Site pressure	37.956 .354 0
3	Atmosphere	1
3a	Reference atmosphere	'USSA'
4	Water vapor	1
5	Ozone	1
6	Gaseous absorption	1
7	Carbon dioxide	370
7a	Extraterrestrial spectrum	0
8	Aerosol model	'S&F Rural'
9	Turbidity	0
9a	Turbidity value	0.084
10	Albedo	29
10b	Tilt albedo	1
10c	Tilt and azimuth	29 22.956 180.
11	Spectral range	280 4000 1.0 1366.1
12	Output	2
12 a	Spectral range to be printed	280 4000 .5
12b	Number of spectral results	8
12c	Specific spectral results	1 2 3 4 5 6 7 8
13	Circumsolar	0
14	Smoothing filter	0
15	Illuminance	0
16	UV	0
17	Solar Geometry	3

Table III: System sensor gains and offsets

Sensor	Gain	offset
UCAP current	9.4943	0.0438
UCAP voltage	15.0909	0.0496
PV voltage	16.9231	0.1191
PV current	10.5769	0.0505

Table IV: 2009 charge cycle statistics

Radiation Estimation Method and Charge Range	Basic Statistics	7-29	7-31	8-13	8-14	8-15
SMARTS ext. short range	Mean	10.01	10.84	9.290	12.54	11.41
	Median	11.21	11.90	9.50	12.59	12.40
	Std. Dev	4.172	3.511	3.481	1.813	3.473
	Sample Size	93	80	84	113	100
	COV	0.42	0.32	0.37	0.14	0.30
SMARTS long range	Mean	13.97	16.51	12.47	15.72	13.52
	Median	14.02	15.52	12.22	16.26	13.68
	Std. Dev	4.641	3.430	4.702	3.389	4.498
	Sample Size	79	20	71	91	75
	COV	0.33	0.21	0.38	0.22	0.33
i vector ext. short range	Mean	10.13	11.15	9.455	12.94	11.90
	Median	11.67	12.61	9.52	13.10	12.89
	Std. Dev	4.241	3.801	3.493	2.075	3.511
	Sample Size	93	80	84	113	100
	COV	0.42	0.34	0.37	0.16	0.30
i vector long range	Mean	13.99	15.58	12.56	15.91	13.79
	Median	14.48	16.06	12.17	15.89	14.26
	Std. Dev	4.619	5.305	4.598	3.596	4.524
	Sample Size	79	20	71	91	75
	COV	0.33	0.34	0.37	0.22	0.32
$I_{bc}$ ext. short range	Mean	11.81	12.45	12.81	12.88	13.65
	Median	12.56	12.43	13.05	13.04	13.44
	Std. Dev	2.744	2.451	2.040	2.437	2.343
	Sample Size	93	80	84	113	100
	COV	0.23	0.19	0.15	0.19	0.17
$I_{bc}$ long range	Mean	16.69	16.88	17.46	16.49	17.45
	Median	16.57	17.76	18.07	16.74	18.32
	Std. Dev	3.286	5.504	2.764	3.942	3.442
	Sample Size	79	20	71	91	75
	COV	0.20	0.33	0.16	0.24	0.20

## SECTION

### 4. RECOMMENDATIONS FOR FUTURE WORK

The following ideas and topics are recommended to continue this research and to address assumptions made in this paper.

- Adjusting the experimental design to account for the effect of the PV modular temperature on the UCAP charge rate is expected to add clarity to the dataset.
- Experiment with the location of the system by collecting several datasets at a variety of locations. Given those results, a prediction model could be tested for the performance of the system at a given location.
- Experiment with various types of renewable energy used to charge the UCAP. For example, wind energy is a function of solar energy and can be harvested through the night un-like solar energy.
- Experiment using several UCAPs in series to characterize the power buffer provided during periods of decreased solar energy.

## APPENDIX

### SCATTERPLOTS OF DATA ON CD-ROM

#### 1. INTRODUCTION

Included with this Thesis is a CD-R, which contains the standard operating procedure (SOP), all raw sensor data, and y/x transformed data collected while the system was operational. All documents have been prepared as Microsoft Word 97-2003 document files. The raw sensor data was prepared as text files. The scatterplots were prepared as Grapher 6 files. An outline of the contents of the CD-R is as follows.

#### 2. CONTENTS

SOP.doc

Raw data

Grapher 6 data files

Excel input data

## REFERENCES

Gilbert, R.O. 1987. *Statistical Methods for Environmental Pollution Monitoring*. John Wiley and Sons, Inc. New York, New York.

Helsel, D.R. & R.M. Hirsch 2002. *Statistical Methods in Water Resources*. US Department of the Interior. US Geological Survey.

Navidi, William (1996). *Statistics for Engineers and Scientists*. McGraw Hill, Boston, Massachusetts.

## VITA

Jenna Vujic was born to Terry Tune and Elizabeth Standfast of Rolla, Missouri. Jenna earned a Bachelor of Science degree in Biological Sciences at the Missouri University of Science and Technology in December 2004. She received a Master's degree in Geological Engineering from the Missouri University of Science and Technology in May 2010.